sciendo

POLISH MARITIME RESEARCH Special Issue 2018 S3 (99) 2018 Vol. 25; pp. 54-60
10.2478/pomr-2018-0112

EXPERIMENT ON PRESSURE CHARACTERISTICS OF SUBMERGED FLOATING TUNNEL WITH DIFFERENT SECTION TYPES UNDER WAVE CONDITION

Qinxi Li[1]
Shuping Jiang[2]
Xiang Chen[3]
[1] School of Civil Engineering, Chongqing Jiaotong University, Chongqing, China
[2] China Merchants Chongqing Communication Research & Design Institute Co., Ltd., Chongqing, China
[3] School of Civil Engineering, Chongqing Three Gorges University, Chongqing, China

ABSTRACT

Submerged floating tunnel (SFT for short) is a special underwater traffic structure, and wave load is one of the main environmental loads of SFT structure. In this paper, the 1:60 physical model test of three kinds of SFT in a two-dimensional wave flume is tested. The effects of random irregular waves on the SFT structure under different wave heights and periods are discussed. The study shows that: (1) Compared with circular and polygonal sections, there are multiple local peaks in the elliptical section during the period. with the increase of wave height, the number of local peaks also increases. It suggests that the rotational moment plays an important role in the elliptical section which has a relatively small depth-width ratio. (2) The position of the maximum and minimum pressure in the three kinds of SFT sections is consistent. Their vertical wave forces are all larger than their horizontal wave forces. The increase of vertical wave force relative to horizontal wave force in polygon section is larger than that in elliptical section, and the difference in the circular section is the smallest. (3) Under the same traffic condition, the wave force of the elliptical and polygon section is smaller, but they are more sensitive to the change of wave height, and the increase is obvious. The distribution of wave force in the circular section is more uniform.

Keywords: Submerged floating tunnel, section type, irregular waves, pressure characteristics, physical test

INTRODUCTION

Submerged floating tunnel (SFT for short) is the only way to maintain the dynamic balance of the water structure by the buoyancy and the cable tension. In some places where it is difficult to build a tunnel or bridge to cross. SFT can be used as a transportation scheme to solve narrow and deep Straits, lakes and rivers. So far, there is still no real SFT in the world.

Although scholars at home and abroad are almost sure that it must be buried under a certain depth of water, the effect of wave force on SFT is negligible. However, there is still a need to study the wave force of the SFT structure. From the project plan, the structure of pure SFT scheme has the water entry section, the transition section and the deep buried section. The first two sections of the SFT structure are affected by the wave force. If the combination of "shield method + submerged floating tunnel method" or "immersed tube method + submerged floating tunnel method" is adopted, the connection position will inevitably exist. The determination of the best connection position also needs to study the exact influence of the depth range on the wave force of the SFT structure. In addition, it is necessary to study the response of the deep fjord wave to the SFT structure, which had great damage and deep influence.

The study of the engineering scheme of the submerged floating tunnel is the first problem in front of the engineer, especially the problem of the type selection of the submerged floating tunnel. Around the form of a submerged floating tunnel section, many countries are aimed at different sea area characteristics and project conditions, a variety of cross section forms are put forward, it includes circular, ellipse and polygons [1]. In 1966, British engineer Mr. Grant proposed the basic idea of building a water submerged floating tunnel in

the water. He proposed a submerged floating tunnel structure with 3 circular concrete pipes with diamond shaped steel shells. In 1984, Italy Archimedes company designed a prestressed concrete pipe structure for the eight sides of Messina strait [2]. Then, a variety of structural schemes have been put forward, such as steel concrete steel sandwich tube section, outer steel tube + inner shell section and pipe joint structure of steel –concrete – steel circular structure section. In 1996, four Norway companies proposed four different submerged floating tunnels with different Anchorage and buoy structures. In 1996, Japan [3] proposed an up and down two highways and rail traffic submerged floating tunnel for the Funka Bay. At the same time, a submerged floating tunnel scheme is proposed for the traffic line of North Japan [4], with circular section of inner concrete and external elliptical shell structure. In 2009, a submerged floating tunnel with an oblique anchorage was put forward in the Sulafjord fjord. In 2016, Norway also designed a double cylindrical structure of submerged floating tunnel in the Sognefjord fjord. Therefore, we have designed three kinds of SFT sections, round, ellipse and polygon, as the alternative for the SFT physical model test.

In the physical model experiment of SFT, The SFT's static water load test was first carried out by a scholar [5–7], he tested the spatial stress distribution of the tube section under the hydrostatic load. A previous researcher [8, 9] carried out the SFT structure section model test and studied the spatial stress and the distribution of the axial force of the anchor cable in the SFT structure under pure flow, but the flow rate in the pool space is not easy to control. The SFT structure test under the uniform flow condition of Venkataramana [10] is more refined, and the random vibration of the SFT model is observed. Japan and South Korea are the long and multi island countries of the coastline. Scholars of the two countries are mainly devoted to the study of the motion characteristics of SFT under the action of waves in the fjord or shallow sea area. A Japanese scholar carried out a model test of a shallow water submerged floating tunnel [11, 12]. It is believed that the tension of the anchor cable increases with the increase of the regular wave period. South Korea's S-H. a group of scholars [13, 14] also studied the hydrodynamic characteristics of SFT under the action of waves through a regular wave physical test in a wave flume. It is found that the anchorage system has an important influence on the movement displacement of the structure. The model test of SFT experienced the development of static water test to pure flow, regular wave and random irregular wave. The test conditions also advance to the single flow to wind and wave water flume, and the large wave water pool test in deep water. Because the regular wave has only one specific period, the test result is generally unstable. Sometimes the resonance result is large, sometimes the result is small, and the irregular wave period has certain distribution, the test result rule is usually relatively stable. Therefore, based on the above three types of SFT section, the structure response of SFT structure under random irregular waves is studied. It provides a reference for the optimization and development of new structural type SFT in the future.

PHYSICAL TEST

TEST EQUIPMENT AND MODEL STRUCTURE

Based on the consistent consideration of the traffic volume, three kinds of bi-directional six lane highway traffic SFT cross section prototype are selected. Figure 1 shows the design sketch of the SFT.SFT is fixed to the bottom of the seabed by the tension leg. The test wave flume is 60 m long, 1.9 m high, and 2 m wide.

In order to obtain reliable wave sequence, the wave elements were calibrated first. In the width of 2.0 m, the flume was divided into two 1.0 m wide flume. The test area was located in the lower half, and the upper half diffuses the reflected waves, as shown in figure 2. When the wave propagates to the test area, a part of the wave will be reflected back after the structure is encountered. A part of the reflected wave is diffused in the parallel flume in the upper half, and finally the energy of the reflected wave is dissipated by the gravel. And the other part is reflected back to the vicinity of the wave-maker. The wave height of the reflected wave is measured by the wave height instrument, and the wave elimination treatment is carried out on the wave guide plate controlled by the computer. Similarly, reflected wave which propagating through the test area are shattered and its energy dissipated by the gravel. Therefore, whether t the wave propagated through the test area or not, the waves are well treated with wave elimination, which will not cause the reflection and superposition of the waves.

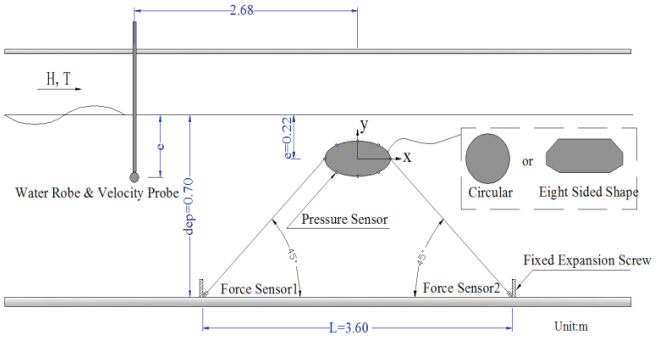

Fig. 1. Experimental parameters and design sketch of the SFT

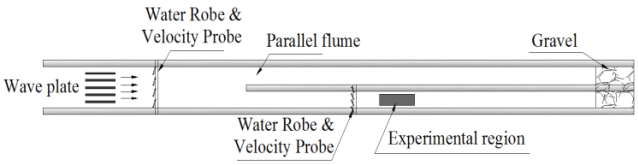

Fig. 2. Schematic diagram of experimental flume arrangement

(a) Top view *(b) Elevation view*

Fig. 3. General situation of experimental device (circle as example)

Tab. 1. Dimensions of main sections of three structural types

Section type	The primary parameter value of the prototype (m)	Prototype section area (m^2)	The main parameter value of the model (cm)	Model section area (cm^2)	Traffic volume
Circular	Diameter = 41.5	1355.0	69.2	3763.9	Bi-directional six lane
Ellipse	Long axis * short axis = 45.0 x 19	671.5	75.0×31.7	1865.3	Bi-directional six lane
Polygon	Height * width = 41.2×13.6	514.2	68.7×22.7	1428.3	Bi-directional six lane

Considering the dimension of the wave flume and the size effect of the hydraulic test, the model test scale is 1:60. The length of the single tube section of the prototype is determined to be 51 m, so the length of the SFT test tube section is determined to be 85 cm. In order to prevent water from entering the pipe section, the pipe joint is in a sealed state during the test. The section parameters of three structural types are given in Table 1. Figure 3 is the general situation of experimental device (circle as example) in the test flume. In order to test the pressure of the surface of the SFT structure under the random wave load, eight pressure sensors are evenly arranged in the circumference of each section. At the same time, in order to test the tension of the anchor cable, four total force sensors are arranged, and the transverse distance between the anchor cables is 70 cm, as shown in Figure 4.

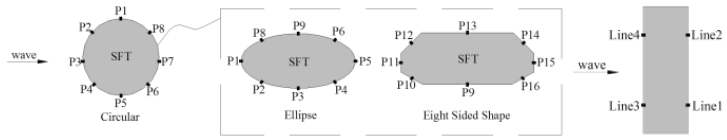

Fig. 4. Measurement point arrangement of sectional pressure and notations of tension legs

SIMILARITY CRITERION

Suspended pipe in water is mainly affected by wave force, ocean currents and earthquakes. The wave force calculated according to the Mirosion equation is mainly the inertial force and the damping force. To simulate the above two types of wave forces, similar designs for dynamic experiments should satisfy Froude similarity and Reynolds similarity. In fact, it is difficult to meet both of them at the same time. According to the ship hydrodynamics experiment and the traditional hydrodynamic experiment experience, the experimental pipe section and the anchor cable should meet the following condition:

PIPE SECTION SIMILARITY

The experimental section is geometrically similar to the prototype of SFT through the 1:60 scale. According to Ge Fei [15]'s study, there exist a suitable range of buoyancy-weight ratio (BWR) value which will lead to less dynamic response and more stability for the SFT, it's called "synergetic range of BWR". Meanwhile BWR determines the range of influence of inclined mooring angle (IMA). When IMA is 45°, BWR=1.3 is adopted to counterweight the structure so that the quality of the pipe section is similar. According to the ship fluid mechanics experiment and the traditional hydrodynamics experiment experience, the experimental material adopts plexiglass.

ANCHOR CABLE SIMULATION

The anchor cable belongs to the non-rigid structure and is simulated by deformation similarity and mass similarity.

The model of anchor rope should be similar to the tension-elongation relationship of the prototype. According to "the wave model test procedure" (Chinese Standard JTJ/T234-2001), the tension-elongation relation of the anchor cable is determined by the following formula (1):

$$T_m = \frac{C_P d_p{}^2 (\Delta S / S)^n}{\lambda^3} \tag{1}$$

Where T_m is model anchor cable tension(N), d_p is diameter of prototype anchor cable(m), C_p is elastic coefficient of prototype anchor cable and usually takes a value of 26.97×10^4 MPa for the anchor cable; $\Delta S/S$ represents relative elongation of prototype anchor cable, S is Initial length of prototype anchor cable; n is the index, and the n value of the cable is recommended for n = 1.5; λ is the model scale, which is 60 in this experiment.

The model of anchor rope is simulated by the combination of steel wire ropes which is basically inelastic (this test range of force measurement) and multi-stage spring steel plates. By varying the length of the spring steel plates to simulate the different tensile – elongation curve, tensile-elongation similarity can be achieved. Meanwhile, the length of anchor cable, the position of the tension legs and anchor angle (45 degrees) of the anchor cable are similar to those of the prototypes. The initial tension of anchor cable is 30kN.

According to "wave model experiment regulations", the quality of cables is similar to that calculated by the following formula (2):

$$W = \frac{C_p d_p{}^2}{\lambda^2} \tag{2}$$

Where W is the mass per unit length of anchor cable (kg/m), d_p is diameter of prototype anchor cable(m), λ is the model scale, which is 60 in this experiment. C_p is mass proportion coefficient of prototype anchor cable in air, and the C_p value of the cable is 3670[kg/(m^2·m)].

WAVE SIMULATION

The wave simulation satisfies the gravity similarity condition, and the irregular wave spectrum adopts JONSWAP spectrum. Thus $s(f)$ is calculated by using formula (3):

$$s(f) = \alpha H_s^{\,2} T_p^{\,-4} f^{-5} \exp\left[-\frac{5}{4}(T_p f)^{-4}\right] \gamma^{\exp\left[-(T_p f-1)/2\sigma^2\right]} \tag{3}$$

Where H_s is significant wave height (m), T_p is the peak period of spectrum (s); γ is the spectral peak parameters, take $\gamma = 3.3$;

$$\alpha = \frac{0.0624}{0.230 + 0.0336\gamma - 0.185(1.9+\gamma)^{-1}}, \quad \sigma = \begin{cases} 0.07 & f \le f_p \\ 0.09 & f \ge f_p \end{cases}$$

Before wave test, the characteristic wave elements are input into the computer to control the wave generator to produce the corresponding irregular wave sequence, so that wave elements meet requirements at the place of model placement.

The experiment adopts the intermittent wave generating method to eliminate the multiple reflections of the wave maker. In this test, each regular wave train has a wave number of about 120, then stops. After the water surface is calm, the next test is carried on. Each trial was repeated 3 times to ensure the reliability of the experimental data.

TEST CONDITIONS AND METHODS

In order to test the effect of wave force on SFT, we assume that the SFT structure is at a shallow water level. We take the immersion depth of the prototype SFT is 6 m. Therefore, the pipe-top of the model is 10 cm from the surface of the water (Immersion depth 10 cm), and the rest of the test parameters is shown in Table 2. The experiment is carried out vertically to the SFT structure in the direction of wave motion, and the test wave is set as a series of irregular wave sequences with different wave heights and different period. The main test parameters of the pressure testing system and the tension test system are shown in Table 3.

Tab. 2. Experimental conditions

Class	parameter	parameter value
Model	Immersion depth	0.1m
	Length of pipe section	0.85m
	Support mode	Flexible anchor cable
	Anchor cable type	steel wire rope
Anchor cable	Diameter of wire rope	2.5mm
	Inclined mooring angle (IMA),	45°
	Wave period	1.5s~2.1s
Wave	Wave height	2cm~6cm

Tab. 3. Main parameters of measurement system

type	Sensor range	Resolution accuracy	Frequency of sampling
Pressure measurement system	10–20/kPa	1%	0.008 seconds / times
Total force measurement system	2~30/kg	1%	0.03 seconds / times

TEST ANALYSIS

Under the same period and different wave heights, wave pressure at wave ward side – time diagram of the three SFT cross sections is shown in Figure 5. When the bi-directional six lanes are adopted, which means that the traffic volume is consistent, the three kinds of cross sections can be compared. Due to the difference of section area, the wave force time history curves of three kinds of cross section show significant difference. The circular section has the largest section area, and its peak pressure in the time history curve is also the largest. Compared to the circular and polygonal sections, the elliptical section has several obvious local peaks in the period. Moreover, with the increase of wave height, the number of local peaks also increases. It suggests that the rotational moment plays an important role in the elliptical section which has a relatively small depth-width ratio. Therefore, the rotation moment of the cross section should be paid more attention to in the structural design.

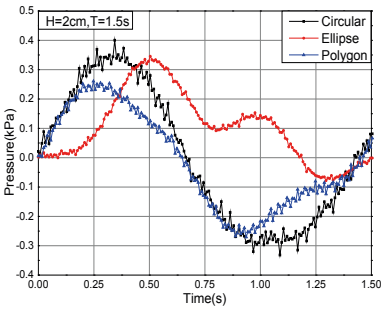

(a) H=2cm, T=1.5s

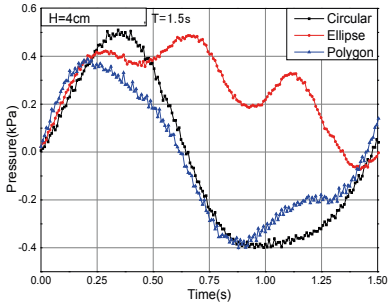

(b) H=4cm, T=1.5s

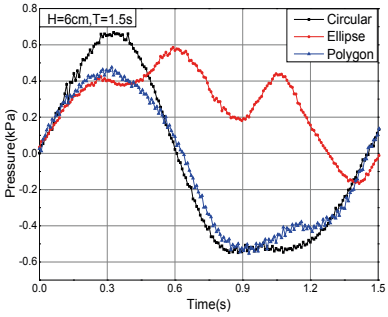

(c) H=6cm, T=1.5

Fig. 5. Wave front pressure at different wave cross sections

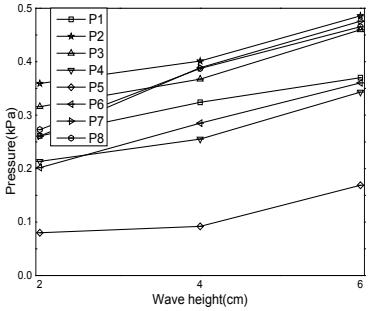

(c) Polygonal cross section

Fig. 6. Circumferential pressure of three cross sections

After changing the experimental period T of the wave, the pressure value will change. It suggests that the pressures still vary with the wave heights. Therefore, we take the period T = 1.5s as an example to illustrate. We select eight measuring points on each section, and then measure the peak value of the pressure at each measuring point. The measurement results are shown in Figure 6. Overall, the peak value of pressure of three SFT sections shows a positive correlation with wave height. Because the position of each sensor on the cross section is different, there is a significant difference the value of pressure. For the circular section, the maximum pressure appears at P2 on the wave front (clockwise 315 degrees), and the minimum pressure appears at P5 (clockwise 180 degrees). The maximum pressure at the elliptical and polygonal sections also occurs at P2, and the minimum pressure appears at P5.

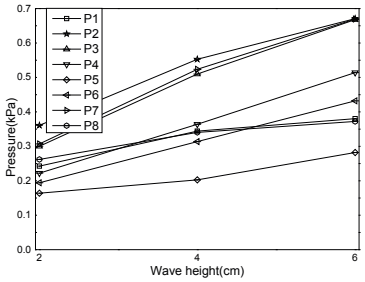

(a) Circular cross-section

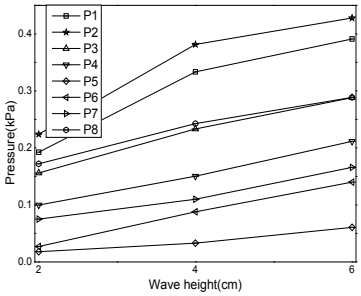

(b) Elliptical cross section

Based on a study, the wave force was evaluated based on the diffraction theory by Boundary Element Method [15, 16]. We got inspiration from it and evaluated vertical and horizontal the wave force by the circumferential pressure obtained experimentally. Taking the period T = 1.5s as an example, the vertical and horizontal wave forces of three kinds of SFT cross sections are given in Figure 7. The vertical and horizontal wave force of three kinds of SFT cross sections are positively correlated with wave height. For circular section, vertical force is larger than horizontal force, 2%~12% [17]. For elliptical section, vertical force is larger than horizontal force, 52%~55%. For polygon section, the vertical force is larger than horizontal force,67~69%. It suggests that the vertical wave forces of the three kinds of cross sections are larger than the horizontal wave forces [18]. Thus, the vertical force should be paid more attention to in the structural design 19]. By comparing the increase values of vertical wave force relative to horizontal wave force on three kinds of cross sections, it is found that the increase of polygon cross section is greater than that of ellipse section while the increase of circular section is the smallest 20]. It is indicated that wave height is one of the important factors affecting wave force, and the sensitivity of elliptical and polygonal sections to wave height change is more obvious than that of circular section [21].

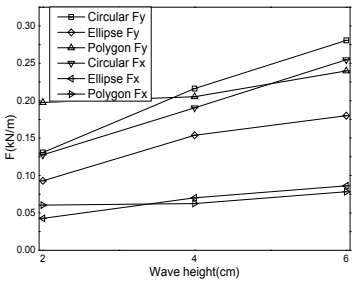

Fig. 7. Vertical and horizontal wave forces of three SFT sections

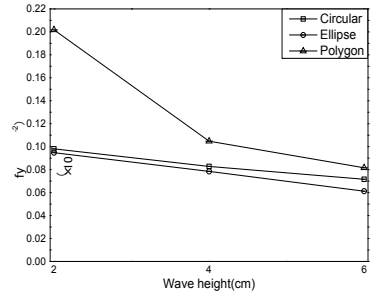

(a)

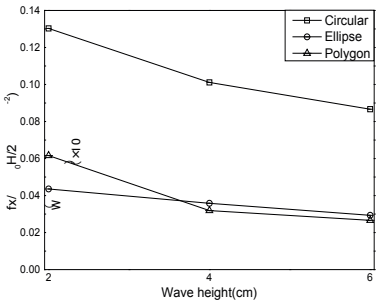

(b)

Fig. 8. Dimensionless wave forces of three SFT sections

In the analysis of wave forces, a scholar proposed the method of dimensionless wave force, that is, the wave force is divided by the water mass and half of the wave height. In Figure 8, the dimensionless results of vertical and horizontal wave forces of three kinds of cross sections are given respectively, and the transverse axis is wave height [22]. As shown in Figure 8, with the increase of wave height, the dimensionless wave force is not linearly increased. On the other hand, the increase of the dimensionless wave force decreases gradually when the wave height is equivalent increased, and the rate of the decrease of the vertical dimensionless wave force and the horizontal dimensionless wave force is almost the same.

CONCLUSIONS

This study carried out physical experiments to investigate the effects of random irregular waves on the SFT structure under different wave heights and periods. This creative result of physical experiment has been summed up as the following aspects.

The pressure of the three SFT sections all increases with the wave height, and the position of the maximum and minimum pressure in the three kinds of SFT sections is consistent. The maximum value appears at P2, the minimum value appears at P5. For elliptical section, there are multiple local peaks during the period. And with the increase of wave height, the number of local peaks also increases. It suggests that the rotational moment plays an important role in the elliptical section which has a relatively small depth-width ratio.

By evaluating the wave force, it is found that the wave forces of the three SFT sections also increases with the wave height. Their vertical wave forces are all larger than their horizontal wave forces. The increase of vertical wave force relative to horizontal wave force in polygon section is larger than that in elliptical section, and the difference in the circular section is the smallest.

Under the same traffic condition, the wave force of the elliptical and polygon section is smaller, but they are more sensitive to the change of wave height, and the increase is obvious. The distribution of wave force in the circular section is more uniform

ACKNOWLEDGMENT

This work was financially supported by the National Ministry of Transport Major Construction Technology Projects "Preliminary Study on Key Technologies of Deep Sea Submerged Floating Tunnel" (Grant No. 2013318740050).

REFERENCES

1. F. Perotti, G. Barbella, and M. D. Pilato, *The dynamic behavior of Archimede's Bridges: Numerical simulation and design implications*, Procedia Engineering, No. 4, pp. 91–98, 2010.

2. G. Martire, B. Faggiano, F. M. Mazzolani, A. Zollo, and T. A. Stabile, *Seismic analysis of a SFT solution for the Messina Strait crossing*, Procedia Engineering, Vol. 4, No. 6, pp. 303–310, 2010.

3. B. Jakobsen, *Design of the Submerged Floating Tunnel operating under various conditions*, Procedia Engineering, Vol. 4, No. 6, pp. 71–79, 2010.

4. S. Kanie, T. Mikami, and Y. Kakuta, *Dynamic Characteristics of Submerged Floating Tunnels Due to Wave Force*, Proceedings of the Japan Society of Civil Engineers, No. 556, pp. 159–168, 2010.

5. B. Faggiano, G. Martire, and F. M. Mazzolani, *Cable Supported Immersed Inversed Bridge: A challenging proposal*, Procedia Engineering, Vol. 4, No. 6, pp. 283–291, 2010.

6. S. Kanie, *Feasibility studies on various SFT in Japan and their technological evaluation*, Procedia Engineering, Vol. 4, pp. 13–20, 2010.

7. Y. Gan, X. Xu, *Three-dimensional degenerate beam element method for stability analysis of thin-walled members*, Journal of Zhejiang University (Engineering Edition), Vol. 37, No. 3, pp. 337–340, 2003.

8. G. Wang, *Numerical analysis and experimental study of SFT structure response under wave current*, Southwest Jiao Tong University, 2008.

9. Y. Qin, *Key technologies of SFT stability under ocean eddy currents*, Southwest Jiao Tong University, 2009.

10. K. Venkataramana, S. Yoshihara, S. Toyota, and Y. Aikou, *Current-induced vibrations of submerged floating tunnels,* Proceedings of the Six International Offshore and Polar Engineering Conference, Vol. 28–31, pp. 111–118, 1996.

11. H. Kunisu, S. Mizuno, Y. Mizuno, and H. Saeki, *Study on Submerged Floating Tunnel Characteristics Under the Wave Condition*, International Society of Offshore and Polar Engineers, 1994.

12. R. Fujita, T. Mikami, T. Yamashita, N. Kawai, and H. Sasaki, *Development of Submerged Floating Tunnels in Shallow Water*, Doboku Gakkai Ronbunshuu B, Vol. 16, pp. 263–268, 2000.

13. S. H. Oh, W. S. Park, S. C. Jang, D. H. Kim, and H. D. Ahn, *Physical experiments on the hydrodynamic response of submerged floating tunnel against the wave action*, Hasanuddin University Press, 2013.

14. S. I. Seo, H. S. Mun, J. H. Lee, and J. Kim, *Simplified analysis for estimation of the behavior of a submerged floating tunnel in waves and experimental verification*, Marine Structures, Vol. 44, pp. 142–158, 2015.

15. Y. Hong, and F. Ge, *Dynamic response and structural integrity of submerged floating tunnel due to hydrodynamic load and accidental load*, Procedia Engineering, Vol. 4, pp. 35–50, 2010.

16. H. Kunisu, *Evaluation of wave force acting on Submerged Floating Tunnels,* Procedia Engineering, Vol. 4, No. 6, pp. 99–105, 2010.

17. B. Q. Li, Z. Li, *The Implement of Wireless Responder System Based on Radio Frequency Technology*, Acta Electronica Malaysia, Vol. 2, No. 1, pp. 15–17, 2018.

18. M. S. Ibrahim, S. Kasim, R. Hassan, H. Mahdin, A. A. Ramli, M. F. Md Fudzee, and M. A. Salamat, *Information Technology Club Management System*, Acta Electronica Malaysia, Vol. 2, No. 2, pp. 01–05, 2018.

19. Z. He, X. Gu, X. Y. Sun, J. Liu, and B. S. Wang, *An Efficient Pseudo-Potential Multiphase Lattice Boltzmann Simulation Model for Three-Dimensional Multiphase Flows,* Acta Mechanica Malaysia, Vol. 2, No. 1, pp. 01–03, 2018.

20. C. Adrian, R. Abdullah, R. Atan, and Y. Y. Jusoh, *Theoretical Retical Aspect in Formulating Assessment Model Of Big Data Analytics Environment,* Acta Mechanica Malaysia, Vol. 2, No. 1, pp. 16–17, 2018.

21. N. Abd Rahman, H. Halim, H. Gotoh, and E. Harada, *Validation of Microscopic Dynamics of Grouping Pedestrians Behavior: From Observation to Modeling and Simulation*, Engineering Heritage Journal, Vol. 1, No. 2, pp. 15–18, 2017.

22. M. A. Hassan, and M. A. Mohd Ismail, *Literature Review for The Development of Dikes's Breach Channel Mechanism Caused by Erosion Processes During Overtopping Failure*, Engineering Heritage Journal, Vol. 1, No. 2, pp. 23–30, 2017.

CONTACT WITH THE AUTHORS

Qinxi Li
e-mail: 494974130@qq.com

School of Civil Engineering
Chongqing Jiaotong University
Chongqing 400074
China